KSTLE International Journal, Vol. 7, No. 2, December 2006, pp. 35-44

Parametric Study on the Design of Turbocharger Journal Bearing - Aeration Effects

Sang Myung Chun†

Department of Automotive Engineering, Hoseo University, Korea

Abstract: Turbocharger bearings are under the circumstance of high temperature, moreover rotated at high speed. It is necessary to be designed overcoming the high temperature. So the type of oil inlet port, the inlet oil temperature and the sort of engine oil should be designed, controlled and selected carefully in order to reduce the bearing inside temperature. In this study, the influence of aerated oil on a high-speed journal bearing is also examined by using the classical thermohydrodynamic lubrication theory coupled with analytical models for viscosity and density of air-oil mixture in fluid-film bearing. Convection to the walls and mixing with supply oil and re-circulating oil are considered. The considered parameters for the study of bubbly lubrication are oil inlet port's type, oil aeration level and shaft speed. It is found that the type of oil inlet ports and shaft speed play important roles in determining the temperature and pressure, then the friction and load of journal bearing at high speed operation. Also, the results show that, under extremely high shaft speed, the high shear effects on aerated oil and the high temperature effects are canceled out each other. So, the bearing load and friction show almost no difference between the aerated oil and pure oil.

Keywords: Aerated oil, Flow mixing, Convective conditions on the walls, High-speed journal bearing, Turbulent Reynolds and energy equations, Oil inlet port

1. Introduction

The shaft of an automotive turbocharger is usually rotated up to 100,000 to 150,000 rpm. This type of the high-speed bearing sustains the shaft by a thin oil film supplied around the shaft through oil supply port. Also the supplied oil reduces the shaft friction and cools down the temperature of the shaft and other parts of the turbocharger. The bearing is so small and rotates at high speed so that it can easily operate under high temperature circumstance. Therefore, it should be designed precisely in durability aspect. Furthermore, it is important to select the type of engine oil because of viscosity sensitivity. So, a parametric study will be carried out in this study in order to find the combinational value of design parameters by numerical analysis.

It is occurred the turbulence inside high-speed bearings as the local Reynolds number reached at the transition region. The turbulent will increase the friction, then results in the noticeable changes of pressure and temperature inside the fluid. Generally, inside rotating bearings, the turbulence occurs as the flow is unstable above 2000 Reynolds number in terms of oil film thickness (h). Or it is easily occurred at the large bearings with a big bearing clearance, and at the fluid flow with lower viscosity. Meanwhile, under turbulence circumstance inside high-speed bearings, the temperature of oil film can sharply increase due to increasing friction, and the temperature variation inside oil film can become severe. Therefore, under such a severe condition of temperature, the variable density and specific heat according to changing temperature should be considered for the design of high speed film bearing [1].

The onset of turbulence in connection with bearings had not become evident until its effects on bearing performance were discovered by a series of experiments [2]. The basic turbulent lubrication theory had been developed by several researchers [3-8]. They handled lubricant as incompressible pure oil.

Meanwhile, a simple empirical viscosity relationship for gas-liquid mixture was found by using a parameter of air-oil volume ratio [9].

The effects of bubble surface tension on density were accounted by assuming that the aerated oil was isoviscous [10]. It was found that the load capacity was virtually unaffected by aeration rate.

The simply density and viscosity models was used for circular pad thrust bearings [11]. They were extended to account for temperature effects. It was found that aeration rate had little effect on load capacity.

An extended Reynolds' equation was derived to account for the fact that aerated oil is non Newtonian [12]. A viscosity model similar to Hayward's [9] was used. It was found that the bearing pressure increases initially with aeration rate, but that the trend is reversed at very high aeration rates when the lubricant starts to behave as a gas.

A first effort at deriving an analytical model for aerated oil viscosity was presented by Nikolajsen [13]. This model predicts an increase in viscosity with increasing aeration level

†Corresponding author; smchun@office.hoseo.ac.kr
Tel: +82-41-540-5816, Fax: +82-41-540-5818

due to the surface tension of the entrained air bubbles. The predicted viscosity increase is confirmed by the experimental findings of Hayward [9]. A corresponding density model for aerated oil is also presented [13]. The mixture theory was applied for aerated oil to one-dimensional Reynolds' equation by assuming that the bearing is long [14]. However, he did not consider energy equation.

The problem of predicting bearing performance when lubricating with bubbly oil could be attacked in two different ways. One could attempt to drive an effective viscosity and density for bubbly oil [13] which, when substituted into the classical Reynolds equation, predicted bearing performance correctly. Another method employed the viscosity of the oil itself, but changed the Reynolds equation to accommodate a mixture lubricant [12].

In a recent paper [15], the Nikolajsen's viscosity and density models [13] were used together with classical Reynolds equation and energy equation to investigate and predict numerically the effects of oil aeration on the performance of a high-speed plane journal bearing with an axial groove. Also, the convective conditions on the walls, the contraction ratio at cavitation region, and the mixing between re-circulating oil and inlet oil were considered together [16-18].

In this paper, the boundary conditions on the bearing wall and the shaft are based on the experimental data. Also, all the considerations mentioned above, for examples, the variable density and specific heat, the effect of oil aeration, the convective wall condition, the contraction ratio at cavitiation region, and the mixing between the recirculating oil and the inlet oil are engaged. It is chosen that types of oil inlet port, oil aeration level, and shaft speed as the design parameters. It is investigated how the parameters effect on the temperature and pressure variation on the oil film, then on the friction loss, the bearing load and the required flow rate.

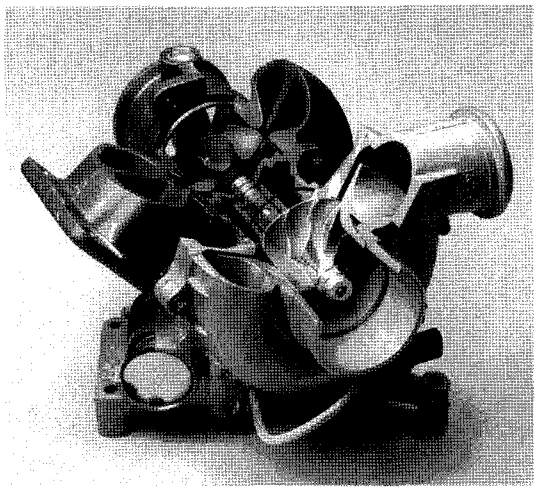

Fig. 1. The cutting view of turbocharger.

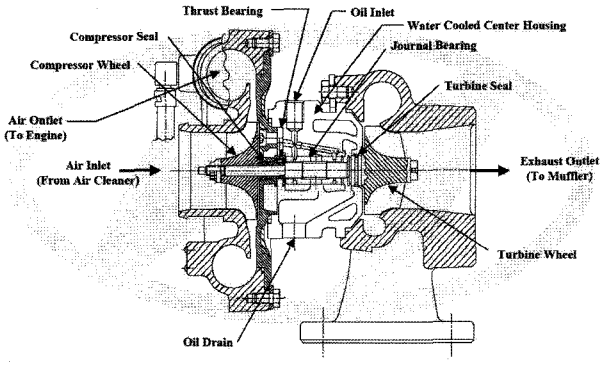

Fig. 2. The cross sectional drawing of turbocharger.

2. Theory

2.1. The characteristics on lubrication environment of a turbocharger bearing

Turbochargers are undertaken very high thermal load owing to making use of the high temperature exhaust gas flowed out from the combustion chamber. The exhaust gas temperature reaches above 750°C, and then the blade of a turbine above 600°C. Even under such a high temperature circumstance, the supplied engine oil has to be able to safely lubricate the bearings supporting the turbine shaft and remove the heat transferred from the shaft. Therefore, higher performance engine oil should be used for the turbocharger engine comparing to that for usual engines. That is, the oil should have better thermal stability, better oxidation stability and good dispersant property in order to circulate the oil better by preventing the viscosity increase and the deposit in engine oil. Also, the oil has lower volatility property in order to prevent exhausting it by evaporation.

Meanwhile, the turbocharger considered in the study is shown in Fig. 1 and Fig. 2. The turbocharger casing temperature reaches around 200~250°C, and the supplied oil temperature 80~100°C during the normal operation. After the supplied oil passes through the bearing inside, the oil temperature increases up to around 120~140°C. So, the shaft temperature may reaches about 40°C higher than that of the supplied oil because the shaft middle area between two bearings is exposed to the oil flowed out from the bearing inside. The temperature of the bush-bearing wall turns out to be the same level of that of the shaft. The supplied oil pressure is normally about 3.5~4.5bar.

2.2. Governing Equations

The Reynolds' equation [3,4] for a steadily loaded journal bearing for finite width may be written as

$$\frac{\partial}{\partial x}\left(\frac{\rho h^3}{\mu} G_x \frac{\partial \bar{p}_g}{\partial x}\right) + \frac{\partial}{\partial z}\left(\frac{\rho h^3}{\mu} G_x \frac{\partial \bar{p}_g}{\partial z}\right) = \frac{U}{2}\frac{\partial(\rho h)}{\partial x} \tag{1}$$

The appropriate values of G_x and G_z are given by the following [5,6] in the range $1{,}000 \le \mathrm{Re} \le 30{,}000$.

$$G_x = \frac{1}{12 + 0.0136\left(\frac{hU}{\nu}\right)^{0.9}} \tag{2}$$

$$G_z = \frac{1}{12 + 0.0043\left(\frac{hU}{\nu}\right)^{0.96}} \tag{3}$$

The steady state two dimensional energy equation [6-8] with heat transfer boundary conditions at the bearing walls may be derived under turbulence conditions as

$$\rho\left\{\left(\frac{Uh}{2} - \frac{h^3}{\mu}G_x\frac{\partial \bar{p}_g}{\partial x}\right)\frac{\partial(C_p\bar{T})}{\partial x} - \frac{h^3}{\mu}G_z\frac{\partial \bar{p}_g}{\partial z}\frac{\partial(C_p\bar{T})}{\partial z}\right\} =$$

$$\tau_c U + \frac{h^3}{\mu}\left\{G_x\left(\frac{\partial \bar{p}_g}{\partial x}\right)^2 + G_z\left(\frac{\partial \bar{p}_g}{\partial z}\right)^2\right\} - (q_{sT} + q_{bT}) \tag{4}$$

where,

$$q_{sT} = H_{sT}(\bar{T} - T_s)$$

$$q_{bT} = H_{bT}(\bar{T} - T_b)$$

The values of H_s and H_b [19] are chosen as shown in Table 3.

In the range $1{,}000 \le \mathrm{Re} \le 30{,}000$, appropriate values of $\bar{\tau}_c$ $(=\tau_c / \frac{\mu U}{h})$ are given by the following (Taylor, 1969; Constantinescu, 1973):

$$\bar{\tau}_c = 1 + 0.0012\left(\frac{\rho Uh}{\mu}\right)^{0.94} \tag{5}$$

The density (kg/m^3) and kinematic viscosity (cst) of pure oil can be expressed by equation (6) and equation (7) with constants, *aa*, *bb* and *cc* which vary depending on the kinds of the oil [20]:

$$\rho_{oil} = 0.0361(aa - 0.000354T_f) \bullet 27680, \tag{6}$$

$$\nu_{oil} = \mu_{oil}/\rho_{oil} = 10^{10^{(bb - cc\log_{10}(Tr))}} - 0.6. \tag{7}$$

where T_f and T_r represent the Fahrenheit temperature and Rankin temperature, respectively. The values of *aa*, *bb*, and *cc* are 0.9070, 9.8500 and 3.5180, respectively, for a current oil. And C_p is the specific heat (J/kg. °C) of oil [21] that may be correlated with Celsius temperature T_c as equation (8).

$$C_p = 1796 + \frac{691}{160}T_c \tag{8}$$

The density (kg/m^3) and dynamic viscosity (Pa · s) of aerated oil can be expressed as shown below [13]. Non-dimensional density can be described as

$$\bar{\rho} = \frac{\rho}{\rho_{oil}} = \frac{(1+\delta)\left(\bar{p}_{oil} + 2\frac{\bar{\sigma}}{\bar{r}}\right)}{\delta + \bar{p}_{oil} + 2\frac{\bar{\sigma}}{\bar{r}}}, \tag{9}$$

where, $\delta = \frac{m_{air}}{m_{oil}} = \frac{(\bar{p}_{oil})_{in} + 2\bar{\sigma}/\bar{r}_{in}}{\frac{3}{4\pi}\left(\frac{\bar{r}_{in}}{d_{in}}\right) - 1}$, $\bar{r} = \frac{r}{c} = \frac{(\bar{p}_{oil})_{in}}{\bar{p}_{oil}}\bar{r}_{in}$

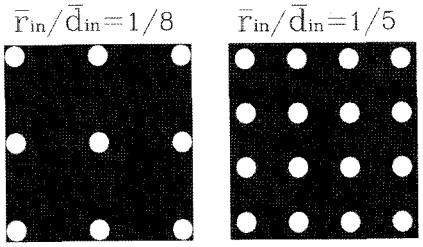

Fig. 3. Oil aeration levels.

$\bar{\sigma} = \sigma/(\rho_{oil}\bar{R}Tc)$, $\bar{\rho} = \bar{\rho}/(\rho_{oil}\bar{R}T)$. $\bar{r}$ is the real root between 0 and $\bar{r}_{in}$ of the polynomial equation

$$\bar{p}_{oil}\bar{r}^3 + 2\bar{\sigma}\bar{r}^2 - [(\bar{p}_{oil})_{in} + 2\bar{\sigma}/\bar{r}_{in}]\bar{r}_{in}^3 = 0.$$

And c is the reference clearance, T is the absolute oil temperature, ρ_{oil} is the density of pure oil, σ is the surface tension of a bubble (N/m), and $\bar{R}$ is the gas constant (J/kg K).

Non-dimensional viscosity [13] can be expressed as:

$$\bar{\mu} = \frac{\mu}{\mu_{oil}} = \bar{\mu}_1 + \bar{\mu}_2 \tag{10}$$

where $\bar{\mu}_1 = \frac{\mu_1}{\mu_{oil}} = \frac{\bar{\rho}}{1+\delta}$, $\bar{\mu}_2 = \frac{\mu_2}{\mu_{oil}} = \Gamma\bar{h}_{in}^{3/2}\bar{r}^{-2}/(\sqrt{\bar{h}})$,

$$\Gamma = \frac{\pi^2\sigma}{\sqrt{2}\mu_{oil}U\bar{r}_{in}^3}\left[\frac{r_{in}}{d_{in}}\right]^3, \quad \bar{h} = \frac{h}{c}, \quad \bar{d} = \frac{d}{c}.$$

And U is the bearing surface speed. d is the distance between bubbles. $\bar{\mu}_1$ represents the viscosity reduction due to the near-zero air viscosity within the bubbles. $\bar{\mu}_2$ represents the viscosity increase due to bubble surface tension. $\bar{r}_{in}/\bar{d}_{in}$ represents oil aeration level illustrated in Fig. 3.

Air volume ratio can be expressed as equation (11) in geometrical aspects of oil aeration level.

$$V = \frac{4\pi}{3A^3} \tag{11}$$

where $A = 1/[2(\bar{r}/\bar{d})_{in}] + 1$.

Note that the density of equation (9) and the viscosity of equation (10) are functions of the absolute oil film pressure $\bar{p}$, whereas Reynolds' equation (1) and energy equation (4) are written as usual in terms of the gage pressure $\bar{p}_g$.

Film thickness, h, can be defined by the expression using bearing coordinates [16]:

$$h = c(1 + \varepsilon\cos(\theta - \varphi)) \tag{12}$$

3. Boundary Conditions

The gage pressure at the ends of a finite length bearing is taken to be equal to the ambient pressure that is defined as being zero. Thus

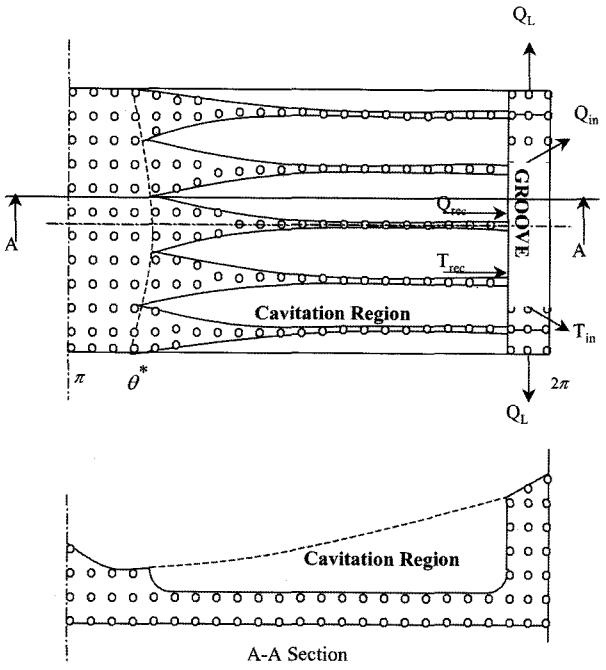

Fig. 4. Diagram of lubricant flow, with Q_{in} the inlet oil flow rate, Q_{rec} the re-circulating flow rate and Q_L the side oil flow rate going through groove land. θ^* is the angle of the beginning of the cavitation region.

$$\bar{p}_{z=\pm L/2} = 0 \tag{13}$$

At the point of film rupture, the pressure boundary conditions are

$$\bar{p} = \frac{\partial \bar{p}}{\partial \theta} = 0 \text{ at } \theta = \theta^* \tag{14}$$

At the ends of bearing, it is reasonable to assume that no heat will be transferred to the surrounding in the axial direction at the ends of the bearing. That is, the oil temperature having come out to the surrounding is assumed the same as of that at the end of the bearing, so

$$q_{z=\pm L/2} = 0. \tag{15}$$

For oil mixing condition, at the groove, the oil temperature is assumed as the mixing temperature between the re-circulating oil and inlet oil as shown on Fig. 2. The detailed expression is defined as

$$T_{mix} = \frac{(Q_{in}-Q_L)T_{in}+L_cQ_{rec}T_{rec}}{(Q_{in}-Q_L)+L_cQ_{rec}}. \tag{16}$$

where L_c is contraction ratio [17] of oil film that defined as

$$L_c(\theta) = \frac{\int_{-L/2}^{L/2}\int_0^{h(\theta^*,z)} u(\theta^*,z)dydz}{\int_{-L/2}^{L/2}\int_0^{h(\theta,z)} u(\theta,z)dydz}. \tag{17}$$

This ratio is the effective wetted width of the bush in the cavitating region. Then the heat transfer coefficient to the bush, adjusted for the reduction of wetting area in the cavitating

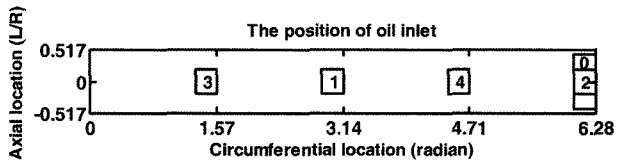

Fig. 5. The various types of oil inlet.

region by the contraction ratio, becomes

$$H_b = L_cH^*_{bo} + (1-L)H_{bg}. \tag{18}$$

where H^*_{bo} is the mixed heat transfer coefficient of aerated oil that is adjusted with air volume ratio (V). It can be expressed that $H^*_{bo} = H_{bo}(1-V) + H_{bg}V$.

The cavitation model of this study is shown on Fig. 4 that shows several oil strips and the shaft covered with oil as usual. It is assumed that the air bubbles mixed with oil are distributed orderly even though the size of air bubble can vary depending on pressure, and that the air bubbles still exist uniformly even inside oil strips. The temperature distribution at air in cavitation region is assumed as the temperature of aerated oil. The gage pressure in cavitation region is zero as mentioned as the boundary condition.

Therefore, generally speaking, for the turbulence treatment of fluid inside bearing, the mixed oil is treated as a sort of virtual oil whose physical properties appear as the mixed viscosity, the mixed density and the specific heat of oil itself. However, the heat transfer to the bearing walls is handled separately from both oil and gas.

In this study, two types of oil inlet port as shown at Fig. 5 are considered. Those are an axial groove and four circular inlet ports. For the convenience of this numerical analysis, a rectangular type of oil port having the similar area compared with that of the original substitutes instead of the circular type of oil port.

4. Calculation of Parameters

The non-dimensional load parameter components $\bar{W}_c$ and $\bar{W}_p$, parallel and normal to the line of centers respectively, are given by:

$$\bar{W}_c = \frac{W_c}{LD}\left(\frac{c}{R}\right)^2\left(\frac{L}{D}\right)/\mu_o N = -\frac{1}{4}\int_0^{2\pi}\int_{-L/D}^{L/D} \bar{P}\cos\theta d\bar{z}d\theta \tag{19a}$$

and

$$\bar{W}_p = \frac{W_p}{LD}\left(\frac{c}{R}\right)^2\left(\frac{L}{D}\right)/\mu_o N = -\frac{1}{4}\int_0^{2\pi}\int_{-L/D}^{L/D} \bar{P}\sin\theta d\bar{z}d\theta \tag{19b}$$

Note that the total load parameter, $\bar{W}$, will be

$$\bar{W} = \sqrt{(\bar{W}_c^2 + \bar{W}_p^2)}. \tag{19c}$$

For turbulent flow, the non-dimensional form of total friction force can be expressed by:

$$\bar{F}_t = \frac{F_t}{LD}\left(\frac{c}{R}\right)\left(\frac{L}{D}\right)/\mu_o N = \frac{1}{4}\int_0^{2\pi}\int_{-\frac{L}{D}}^{\frac{L}{D}}\left(G_x\frac{H}{2}\frac{\partial \bar{H}}{\partial \theta} + \bar{\tau}_c\bar{\mu}\frac{2\pi}{H}\right)d\bar{z}d\theta \tag{20}$$

The frictional torque is equal to friction force multiplied by the radius of a bearing and the frictional power loss is friction force multiplied by the velocity of the bearing shaft.

The non-dimensional axial leakage loss, equal to the required flow, due to the turbulent flow inside a bearing is expressed by:

$$\bar{Q}_{zt} = \frac{Q_{zt}}{NcR^2} = \int_0^{2\pi} -G_z\frac{H^3}{\bar{\mu}}\frac{\partial \bar{P}}{\partial \bar{z}}\bigg|_{\bar{z}=\pm L/D} d\theta \tag{21}$$

5. Computation

The turbulent Reynolds and the energy equations with turbulent similarity parameters have been solved by finite difference method using relaxation factors. Here, over-relaxation factors are used for solving Reynolds equation and under-relaxation factors for solving energy equation. The central finite difference technique is applied for the non-dimensional Reynolds equation. The backward difference scheme in the circumferential direction, and backward and forward difference schemes in the axial direction are used for the non-dimensional energy equation.

In order to create finite difference model in the cavitation region, the total width of oil strips are divided by total numbers of meshes in z-direction, then the small oil strip is allocated at each node. So it is assumed that the oil strip exits at each node.

In this study, the grid used comprises 49 × 17 nodes. Finer grids with double the points in each direction have been tried with no noticeable difference in the results. In addition variable grid size mesh has been utilized to provide greater detail in regions with rapid changes in temperature and pressure without noticeable difference in the results.

With the pressure and temperature distributions thus specified, the load, friction and axial leakage parameters can then be computed from equation (19c), (20) and (21).

6. Results and discussion

6.1. The specification of a bearing and engine oil

The bearing geometry parameters and the lubricant properties used are summarized in Table 1. Two bearings with one axial groove and four circular inlet ports respectively, are examined. The basic algorithm of a numerical model used for this study had been verified by Chun [18].

During operating the considered engine under the condition of wide open throttling on a dynamometer, the volume percent of air in the engine oil varies as changing the shaft speed. This volume percent of aerated oil is corresponding to aeration level. After passing through an oil filter, the oil air bubble size is appeared as about 0.02 mm (20 μm).

In this study, the aeration levels, $\bar{r}_{in}/\bar{d}_{in}$, investigated are 1/12, 1/10, 1/8, 1/7, 1/6 and 1/5 for considering various engine operating conditions. These values can be expressed as air volume ratio, V, as 0.0122, 0.0194, 0.0335, 0.0460, 0.0655 and 0.0977 respectively. And the size of an air bubble, r_{in} is fixed with 20 μm.

Table 1. Journal bearing operating conditions

Bearing diameter	D = 7.85 mm
Bearing length	L = 4.06 mm
Radial clearance	C = 1 μm
Eccentricity ratio	ε = 0.1
Rotational speed	N = 10,000-150,000 rpm
Lubricant viscosity at 40°C (Oil A)	μ_o = 0.0646 Pa.s
Lubricant density at 40°C (Oil A)	ρ_o = 881.08 Kg/m^3
Surface tension	σ = 0.0365 N/m
Lubricant specific Heat at 40°C	C_o = 1968.75 J/kg °C
Convective heat transfer coefficient of lubricant to bush	H_{boT} = 8700 W/m^2 °C
Convective heat transfer coefficient of air to bush	H_{bgT} = 3400 W/m^2 °C
Convective heat transfer coefficient of lubricant to shaft	H_{sT} = 8700 W/m^2 °C
Bush and shaft temperature	$T_{b,s}$ = 140 °C
Inlet lubricant temperature	T_{in} = 100 °C
Inlet Lubricant Pressure	P_{in} = 4.0 × 10^5 Pa
Axial Groove Width	7.5° (1 grid size)

Meanwhile, the viscosity of the engine oil (Oil A) considered here is shown on Fig. 6. The grade of Oil A is SAE 10W40 with the viscosity index 141 and the flash point 220°C.

6.2. The effects of the type of oil inlet ports and engine oils

The calculated pressure and temperature distributions are shown on Fig. 7 to Fig. 10 for the bearings both with an axial groove and with four circular inlet ports. With the axial groove, the pressure in aerated oil film results in partly raising up to 6bar and the temperature decreasing around 3.5~10°C comparing to those in pure oil. With four circular inlet ports, the pressure in aerated oil film also results in partly raising up to 6bar, but the temperature increasing about 3°C comparing to those in pure oil.

Therefore, as a reference, the non-dimensional load parameter in case of the axial groove increases from 2.106 to 2.314 if some air is entrained in the engine oil. The non-dimensional load parameters increase from 0.021 to 0.022. The non-dimensional axial leakage parameter decreases from 0.120 to 0.116. In case of four circular oil inlet ports, the friction parameter decreases from 2.608 to 2.564. The load parameter decreases from 0.020 to 0.018. The axial leakage decreases from 0.332 to 0.326.

As you can see, the oil film temperature in the bearing with an axial groove is about 55°C higher than that with four circular inlet ports. Under such a high temperature, the shear stress of air bubble diminishes. Then the temperature variation in aerated oil drops comparing to that in pure oil. Finally, the load and friction parameter in aerated oil can increase comparing to those of pure oil. On the contrary, under lower temperature, the shear stress of air bubble increases. Then the temperature variation in aerated oil rises comparing to that in

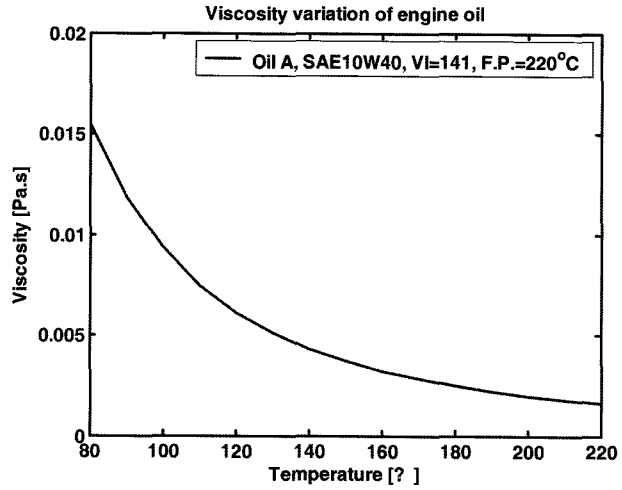

Fig. 6. Engine oil viscosity at various temperatures.

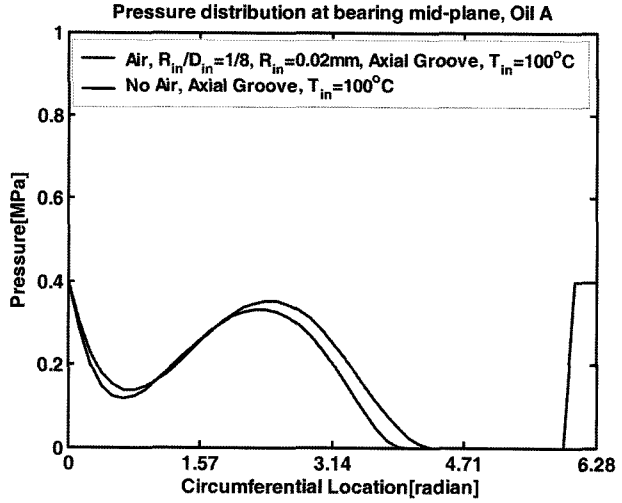

Fig. 7. Pressure distribution at the middle of a bearing plane, Oil A @ 150,000 rpm.

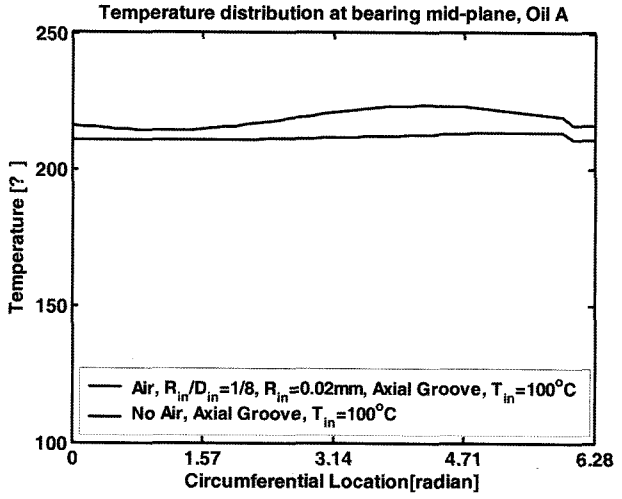

Fig. 8. Temperature distribution at the middle of a bearing plane, Oil A @ 150,000 rpm.

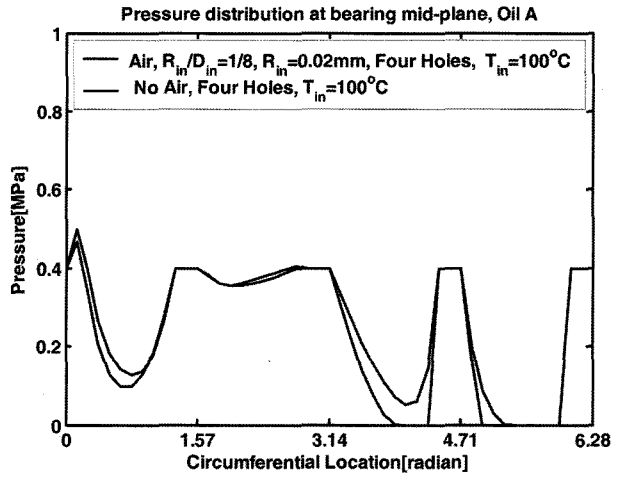

Fig. 9. Pressure distribution at the middle of a bearing plane, Oil A @ 150,000 rpm.

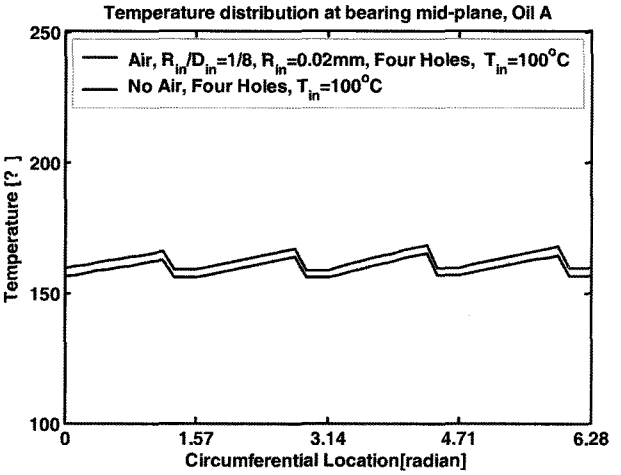

Fig. 10. Temperature distribution at the middle of a bearing plane, Oil A @ 150,000 rpm.

pure oil. Finally, the load and friction parameter in aerated oil can decrease comparing to those of pure oil. Therefore, under extremely high temperature, it can be said that the effect of air bubbles on bearing load is less than that in pure oil.

6.3. The effects of aeration levels

The pressure and temperature distributions of oil film with four circular inlet ports are plotted in Fig. 11 and Fig. 12. As increasing the aeration level, the pressure and temperature usually increase gradually at 150,000rpm of the shaft speed. Unusually, with the aeration level of 1/5 (9.8 volume%), the pressures at the leading area of the bearing sharply increase. But, the temperatures decrease about 3°C comparing to that in case of the aeration level of 1/6 (6.6 volume%). This is because the shear of air bubbles with higher aeration levels plays more important roles in the oil film lubrication comparing to the role of high temperature due to the high shaft speed.

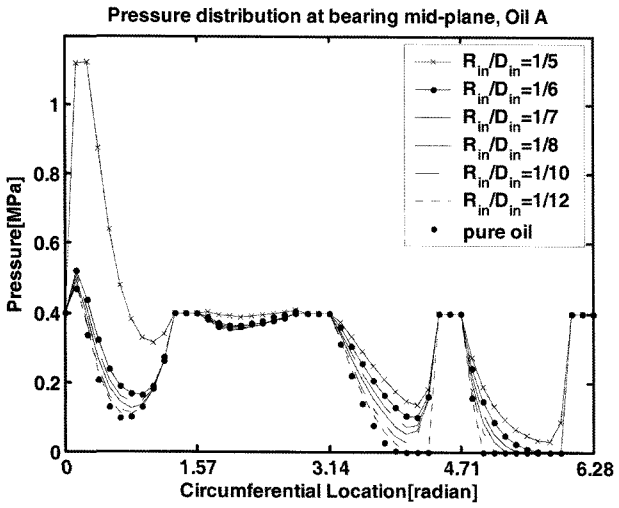

Fig. 11. Pressure distribution at the middle of a bearing plane, Oil A @ 150,000 rpm.

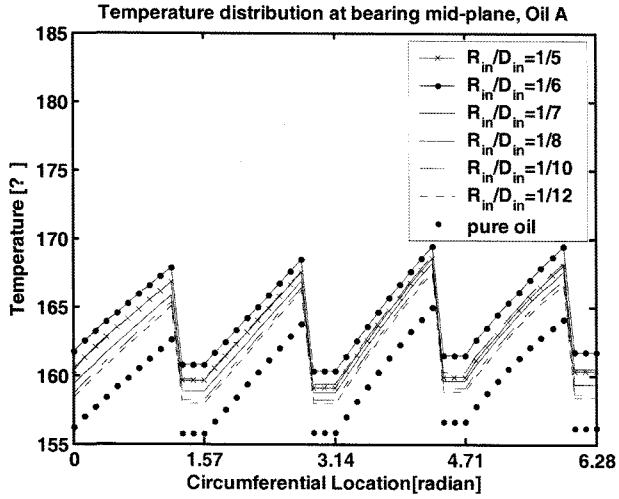

Fig. 12. Temperature distribution at the middle of a bearing plane, Oil A @ 150,000 rpm.

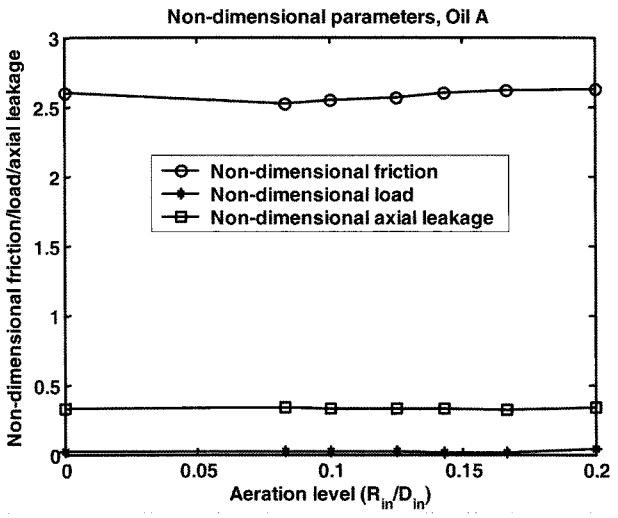

Fig. 13. Non-dimensional parameters' distribution, Oil A @ 150,000 rpm.

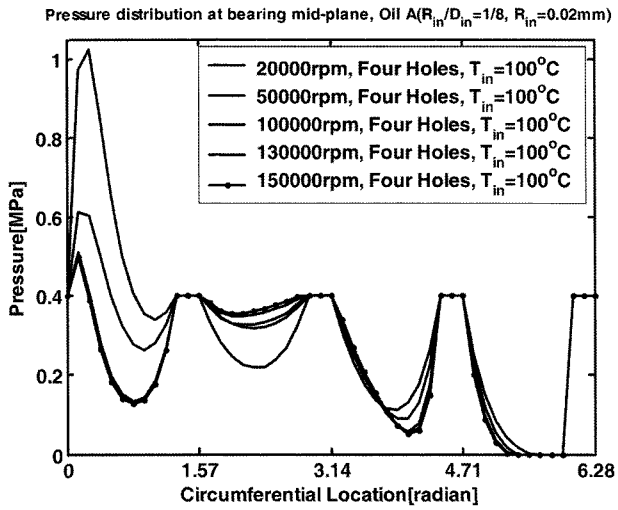

Fig. 14. Pressure distribution at the middle of a bearing plane at various shaft revolutions, Oil A, R_{in}/D_{in}=1/8.

The non-dimensional parameters varying with changing aeration level are shown on Fig. 13. The friction parameter at the aeration level, 1/12 is slightly reduced compared with that of pure oil. This is because the pressure distributions are almost same, but the viscosity at pure oil increases due to much lower temperature. Then, the friction parameter increases as increasing aeration level. The load parameter are shown almost same till the aeration level is 1/6, but the load parameter increases at aeration level 1/5 due to high shear from more air bubbles. Meanwhile, the axial leakage turns out to be almost same as changing aeration level.

6.4. The effects of shaft speeds

The pressure and temperature distributions of oil film with changing the shaft speed are shown on Fig. 14 and Fig. 16. The compared plots between the results in pure oil and in aerated oil are shown on Fig. 15 and Fig. 17.

The oil film pressure at the front area of the bearing increases as increasing the shaft speed up to 50,000 rpm. Above 50,000 rpm, on the contrary, the pressure decreases due to big increase on oil film temperature as shown Fig. 16. As increasing the shaft speed, the increment in oil film temperature turns out to be higher. For example, as the shaft speed increases from 100,000 rpm to 130,000 rpm, the increment is about 6°C. Meanwhile, as increasing from 20,000 rpm to 50,000 rpm, the increment is about 3°C. Comparing the effects of pure oil and aerated oil, the pressure and temperature in the oil film of aerated oil increase slightly more than those of pure oil. The higher the shaft speed, the more the differences in pressure and temperature between pure oil and aerated oil due to the high shear.

The calculated non-dimensional parameters for both pure oil and aerated oil are shown on Fig. 18. As we can see, as increasing the shaft speed, the values of parameters decrease. At comparatively lower speed of the shaft, the friction parameters related with aerated oil turns out to be higher than

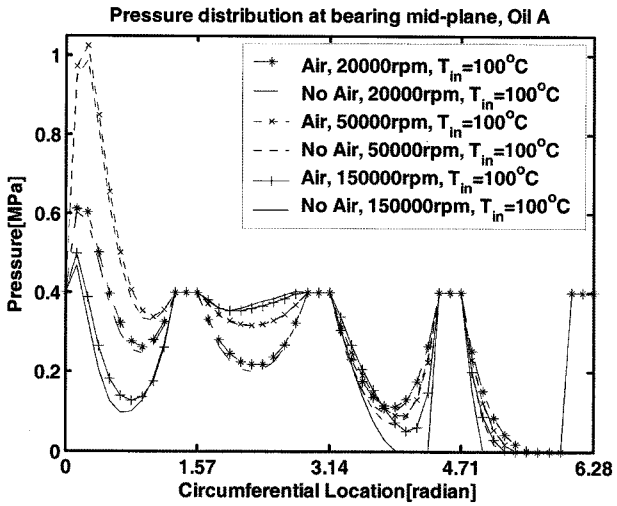

Fig. 15. Pressure distribution at the middle of a bearing plane at various shaft revolutions, Oil A, No air & R_{in}/D_{in}=1/8.

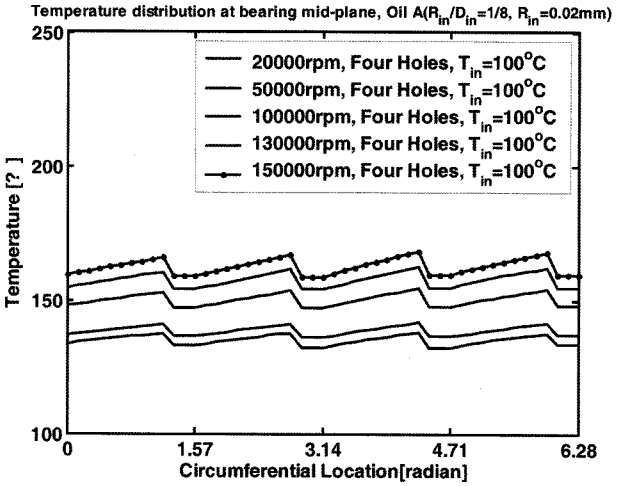

Fig. 16. Temperature distribution at the middle of a bearing plane at various shaft revolutions, Oil A, R_{in}/D_{in}=1/8.

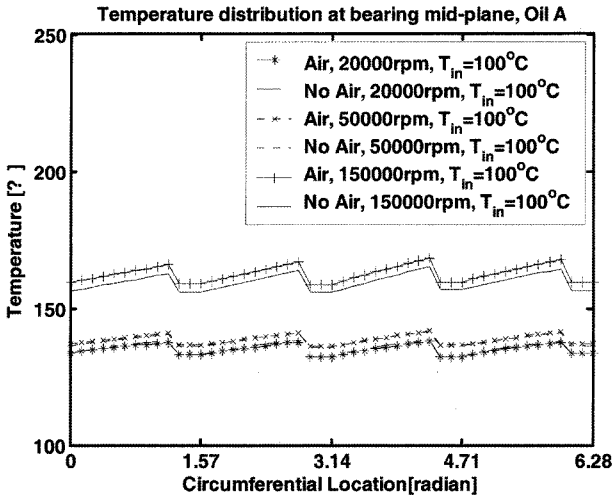

Fig. 17. Temperature distribution at the middle of a bearing plane at various shaft revolutions, Oil A, No air & R_{in}/D_{in}=1/8.

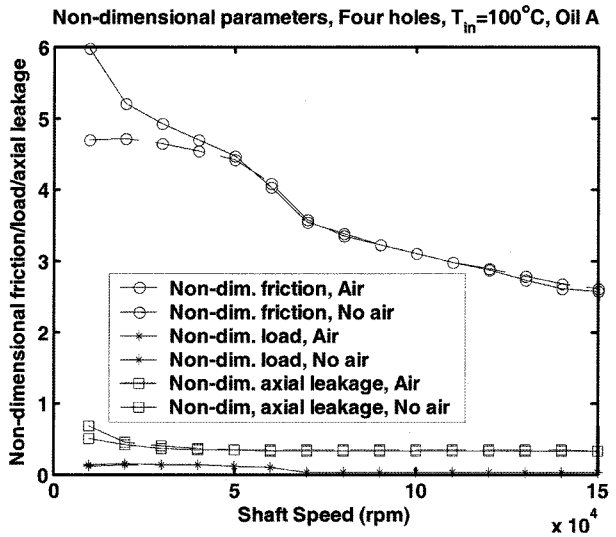

Fig. 18. Non-dimensional parameters' distribution, Oil A, R_{in}/D_{in}=1/8.

those for pure oil, the load parameters be slightly higher than those for pure oil, and the axial leakage parameters be lower than those for pure oil. Under extremely high shaft speed, the high shear effects on aerated oil and the high temperature effects are canceled out each other. So, the bearing load and friction show almost no difference between the aerated oil and pure oil.

Conclusions

As the results of this study, it is concluded that:

Under extremely high temperature, the shear stress of air bubble diminishes. Then the temperature variation in aerated oil drops comparing to that in pure oil. Finally, the load and friction parameter in aerated oil can increase comparing to those of pure oil.

As increasing the aeration level, the pressure and temperature usually increase at 150,000 rpm of the shaft speed. Unusually, with the aeration level of 1/5, the pressures at the leading area of the bearing increase sharply. But, the temperatures decrease about 3°C comparing to that in case of the aeration level of 1/6. This is because the shear of air bubbles with higher aeration levels plays more important roles in the oil film lubrication comparing to the role of high temperature due to the high shaft speed.

The higher the shaft speed, the more the differences in pressure and temperature between pure oil and aerated oil due to the high shear.

As increasing the shaft speed, the values of parameters decrease. At comparatively lower speed of the shaft, the friction parameters related with aerated oil turns out to be higher than those for pure oil, the load parameters be slightly higher than those for pure oil, and the axial leakage parameters be lower than those for pure oil. Under extremely high shaft speed, the high shear effects on aerated oil and the high

temperature effects are canceled out each other. So, the bearing load and friction show almost no difference between the aerated oil and pure oil.

Acknowledgments

This research was supported by the Academic Research fund of Hoseo University in 2005 (Project No.: 20050272).

Nomenclature

c = radial clearance between journal and its bearing (m)
C_p = specific heat of lubricant (kJ/kg°C)
d = distance between two bubbles (m)
d_{in} = distance between two bubbles at inlet condition (m)
$\bar{d}$ = non-dimensional distance between two bubbles = d/c
$\bar{d}_{in}$ = non-dimensional distance between two bubbles at inlet condition = d_{in}/c
D = bearing diameter (m)
e = eccentricity(the offset distance between journal and bearing centers)
F = friction force
$\bar{F}$ = non-dimensional friction force = (F/LD) (c/R)/(μ_oN)(L/D)
h = oil film thickness (m)
$\bar{h}$ = non-dimensional film thickness = h/c
h_{in} = oil film thickness at inlet (m)
$\bar{h}_{in}$ = non-dimensional film thickness at inlet = h_{in}/c
$H_{bT,\,sT}$ = convective heat transfer coefficient at bush and shaft (W/m²°C)
L = bearing length (m)
N = rotational speed (rpm)
$\bar{p}$ = mean absolute pressure for turbulent flow (Pa)
p_g = mean gage pressure for turbulent flow (Pa)
$\bar{p} = \bar{p}/(\rho_{oil}\bar{R}T)$
$\bar{P}$ = non-dimensional mean pressure $(\bar{p}_g(c/R)^2/\mu_o N)$
$\bar{P}$ = non-dimensional effective pressure $(H^{3/2}\bar{P}/\bar{\mu}^{1/2})$
P_{in} = inlet gage pressure (Pa)
$q_{bT,\,sT}$ = turbulent heat transfer to the bush and shaft (W)
Q_{zt} = lubricant side leakage (m³/s)
$\bar{Q}_{zt}$ = non-dimensional lubricant side leakage (Q_{zt}/NcR^2)
r = bubble radius (m)
r_{in} = bubble radius at inlet condition (m)
$\bar{r}$ = non-dimensional bubble radius = $\frac{r}{c}$
$\bar{r}_{in}$ = non-dimensional bubble radius at inlet condition = r_{in}/c
R = journal bearing radius (m)
$\bar{T}$ = mean temperature for turbulent flow(°C)
$\bar{T}$ = non-dimensional mean temperature

$$\frac{\rho C_o (c/R)^2}{2\pi\mu_o N}(\bar{T} - T_{in})$$

T_{in} = inlet oil temperature (°C)
T_b = temperature of the bush (°C)
T_s = temperature of the shaft (°C)
T_f = Fahrenheit temperature (°F)
T_r = Rankin temperature (°R)
U = speed of journal (m/s)
V = air volume fraction
W = applied load
$\bar{W}$ = non-dimensional load parameter

$$\left(\frac{W}{LD}\left(\frac{c}{R}\right)^2\left(\frac{L}{D}\right)/(\mu_o N)\right)$$

x, z = coordinates of circumferential and axial directions, respectively
θ, z = non-dimensional coordinates ($\theta = x/R, \bar{z} = z/R$)
δ = air/oil mass ratio
ε = eccentricity ratio = e/c
μ = aerated oil viscosity (Pa.s)
μ_o = inlet aerated oil viscosity (Pa.s)
μ_{oil} = pure oil viscosity (Pa.s)
$\bar{\mu} = \mu/\mu_{oil}$
ρ = aerated oil density (kg/m³)
ρ_{oil} = pure oil density (kg/m³)
$\bar{\rho}$ = non-dimensional density = ρ/ρ_{oil}
σ = surface tension of air bubble (N/m)
$\bar{\sigma} = \sigma/(\rho_{oil}RTc)$
v = aerated oil kinematic viscosity (cSt)
v_{oil} = pure oil kinematic viscosity (cSt)
φ = attitude angle, i.e., angle between the line of centers and the axial plane containing the load vector

References

1. Chun, S. M., "Thermohydrodynamic Lubrication Analysis of High-Speed Journal Bearing Considering Variable Density and Variable Specific Heat," Tribology International, Vol. 37, No. 5, pp. 405-413, 2004.
2. Wilcock, D. F., "Turbulence in High Speed Journal Bearing," *Trans. of the ASME*, Vol. 72, pp. 825-834, 1950.
3. Constantinescu, V. N., "Theory of Turbulent Lubrication," *Proc. Int. Symp. on Lubrication and Wear*, University of Houston, pp. 153-213, 1965.
4. Ng, C. W. and Pan, C. H. T., "A Linearized Turbulent Lubrication Theory," *Trans. of the ASME, J. of Basic Engineering*, Vol. 87, pp. 675-688, 1965.
5. Taylor, C. M., "Turbulent Lubrication Theory Applied to Fluid Film Bearing Design," *Proc. Inst. Mech. Engrs.*, Vol. 184, Part 3L, pp. 40-47, 1969-1970.
6. Constantinescu, V. N., "Basic Relationships in Turbulent Lubrication and Their Extension to Include Thermal Effects," *Trans. of the ASME, J. of Lubrication Technology*, Vol. 95, pp. 147-154, 1973.
7. Safar, Z. and Szeri, A. Z., "Thermohydrodynamic Lubrication in Laminar and Turbulent Regimes," *Trans. of the ASME, J. of Lubrication Technology*, Vol. 96, pp. 48-57, 1974.
8. Szeri, A. Z., *Tribology: Friction, Lubrication and Wear*, Chapter 5, "Turbulence, Inertia, and Thermal Effects in Fluid Film Bearings," Hemisphere Publishing Corp., pp. 229-294, 1980.
9. Hayward, A. T. J., "The viscosity of bubbly Oil", *National*

Engineering Laboratory, Fluids Report No. 99, Glasgow, U. K, 1961.
10. Smith, E. H., "The Influence of Surface Tension on Bearings Lubricated With Bubbly Liquids", *Trans. of the ASME, Jour. of Lub. Tech.*, vol. 102, pp. 91-96, 1980.
11. Abdel-Latif, L. A., Peeken, H. and Benner, J., "Thermo-hydrodynamic Analysis of Trust-Bearing With Circular Pads Running on Bubbly Oil (BTHD-Theory)", *Trans. of the ASME, Jour. of Trib.*, vol. 107, pp. 527-537, 1985.
12. Chamniprasart, K., Al-Sharif, A., Rajagopal, K. R. and Szeri, A. Z., "Lubrication with Binary Mixtures: Bubbly Oil", *Trans. of the ASME, Jour. of Trib.*, vol. 115, pp. 253-260, 1993.
13. Nikolajsen, J. L., "Viscosity and Density Models for Aerated Oil in Fluid-Film Bearings", *STLE, Tribology Transactions*, vol. 42, no. 1, pp. 186-191, 1999.
14. Nikolajsen, J. L., "The Effect of Aerated Oil on the Load Capacity of Plain Journal Bearing", *STLE, Tribology Transactions*, vol. 42, no. 1, pp. 58-62, 1999.
15. Chun, S. M., "A Parametric Study on Bubble Lubrication of High-Speed Journal Bearings," Tribology International, Vol. 35, No. 1, pp. 1-13, 2002.
16. Chun, S. M. and Lalas, D. P., "Parametric Study of Inlet Oil Temperature and Pressure for a Half-Circumferential Grooved Journal Bearing," *STLE Tribology Transaction,* Vol. 35, no. 2, pp. 213-224, 1992.
17. Boncompain, R., Fillon, M. and Frene, J., "Analysis of Thermal Effects in Hydrodynamic Bearings," *Trans. of the ASME, Jour. of Trib.*, Vol. 108, pp. 219-224, 1986.
18. Chun, S. M., "Study on Mixing Flow Effects in a High-Speed Journal Bearing," Tribology International, vol. 34, no. 6, pp. 397-405, 2001.
19. Gazley, C. Jr., "Heat-Transfer Characteristics of the Rotational Axial Flow Between Concentric Cylinders," *Trans. of the ASME*, Vol. 80, No.1, pp. 79-90, 1958.
20. Lin, H. S., "Viscosity of Motor Oil," *Federal Mogul, Engineering Report*, 1981.
21. Holman, J. P., *Heat Transfer*, McGraw-Hill, Inc., pp. 641, 1986.